Dust in the Local Group

Aigen Li[1], Shu Wang[2], Jian Gao[2], and B.W. Jiang[2]

Abstract How dust absorbs and scatters starlight as a function of wavelength (known as the interstellar extinction curve) is crucial for correcting for the effects of dust extinction in inferring the true luminosity and colors of reddened astrophysical objects. Together with the extinction spectral features, the extinction curve contains important information about the dust size distribution and composition. This review summarizes our current knowledge of the dust extinction of the Milky Way, three Local Group galaxies (i.e., the Small and Large Magellanic Clouds, and M 31), and galaxies beyond the Local Group.

1 Introduction

Interstellar dust is an important constituent of the Milky Way (MW) and external galaxies although it makes up only about 0.1% of the visible matter of a typical galaxy. Understanding dust and its role in the universe are very important. Virtually all observations of astrophysical objects and their physical processes are affected by the presence of dust either within the system being studied or along its line of sight. Dust absorbs and scatters starlight efficiently in the ultraviolet (UV), optical and near infrared (IR) wavelength range. It is the dominant opacity source for continuum photons with wavelengths longward of the ionization edge of hydrogen. In order to infer the intrinsic properties (e.g., luminosity, color, spectral energy distribution) of an astrophysical object, it is crucial to correct for the effects of dust extinction — the sum of absorption and scattering. Correcting for dust extinction is also essential for inferring the stellar content of a galaxy, or the history of star formation in the universe. The uncertainty in the correction for dust extinction currently dominates the uncertainty in the inferred star formation rate in high-z galaxies (see Madau & Dickinson 2014).

1. Department of Physics and Astronomy, University of Missouri, Columbia, MO 65211, USA ·
2. Department of Astronomy, Beijing Normal University, Beijing 100875, China

Dust absorbs and scatters starlight differently at different wavelengths, often with shorter-wavelength (blue) light more heavily obscured than longer-wavelength (red) light. Therefore, dust controls the appearance of a galaxy by dimming and reddening the starlight in the UV and optical (e.g., see Block & Wainscoat 1991, Block et al. 1994, Block 1996). Dust re-radiates the absorbed UV/optical stellar photons at longer wavelengths. Nearly half of the bolometric luminosity of the local universe is reprocessed by dust into the mid- and far-IR (Dwek et al. 1998).

Dust is an important agent of the galactic evolution. Dust plays an important role in interstellar chemistry by providing surfaces for the formation of the most abundant molecule (i.e., H_2) and by reducing the stellar UV radiation which otherwise would photodissociate molecules. The far-IR radiation of dust removes the gravitational energy of collapsing clouds, allowing star formation to occur. Dust dominates the heating of interstellar gas through photoelectrons (Weingartner & Draine 2001a).

In this review we will focus on dust extinction. The study of interstellar extinction has a long history (see Li 2005). As early as 1847, Wilhelm Struve already noticed that the apparent number of stars per unit volume of space declines in all directions receding from the Sun. He attributed this effect to interstellar absorption. From his analysis of star counts he deduced an visual extinction of $\sim 1\,\mathrm{mag\,kpc}^{-1}$. In 1904, Jacobus Kapteyn estimated the interstellar absorption to be $\sim 1.6\,\mathrm{mag\,kpc}^{-1}$, in order for the observed distribution of stars in space to be consistent with his assumption of a constant stellar density (see van der Kruit 2014). This value was amazingly close to the current estimates of $\sim 1.8\,\mathrm{mag\,kpc}^{-1}$ (see Li 2005).

How the interstellar extinction A_λ varies with wavelength λ — known as the "interstellar extinction law" or "interstellar extinction curve" — is one of the primary sources of information about the dust size distribution, and the extinction spectral features provide direct information on the dust composition (Draine 2003). The interstellar extinction curve is most commonly determined using the "pair method" which compares the spectrum of a reddened star with that of an unreddened star of the same spectral type (see Appendix 1 in Li & Mann 2012). This method, first used by Bless & Savage (1970), has since been used extensively to deduce the extinction curves for a large number of Galactic sightlines (see Valencic et al. 2004 and references therein). However, direct measurements of extragalactic UV extinction using individual reddened stellar sightlines are still limited to three Local Group galaxies: the Small Magellanic Cloud (SMC), the Large Magellanic Cloud, and M 31 (see Clayton 2004). In galaxies beyond the Local Group, individual stars can not be observed. Various approaches other than the "pair method" have been taken to determine the extinction curves.

In §2 we summarize our current knowledge of the UV, optical and IR extinction properties of the MW. The extinction curves of the SMC, LMC, M 31 are respectively discussed in §3, §4, and §5. We summarize in §6 the approaches to determining the extinction curve for dust in galaxies where individual stars cannot be resolved. We will not discuss the dust thermal IR/mm emission. The importance of the dust thermal emission of the MW (see Draine & Li 2001, Li & Draine 2001, Li 2004, Jones et al. 2013), the SMC/LMC (Li & Draine 2002; Galliano et al. 2011; Gordon et al. 2011, 2014; Meixner et al. 2010, 2013), and other galaxies (e.g., see Draine

& Li 2007, Draine et al. 2007) cannot be over-emphasized. A simultaneous investigation of the interstellar extinction, scattering, polarization and thermal emission would place powerful constraints on the nature of the dust (e.g., see Li & Greenberg 1997, 1998; Block et al. 1997; Block & Sauvage 2000; Hensley & Draine 2014).
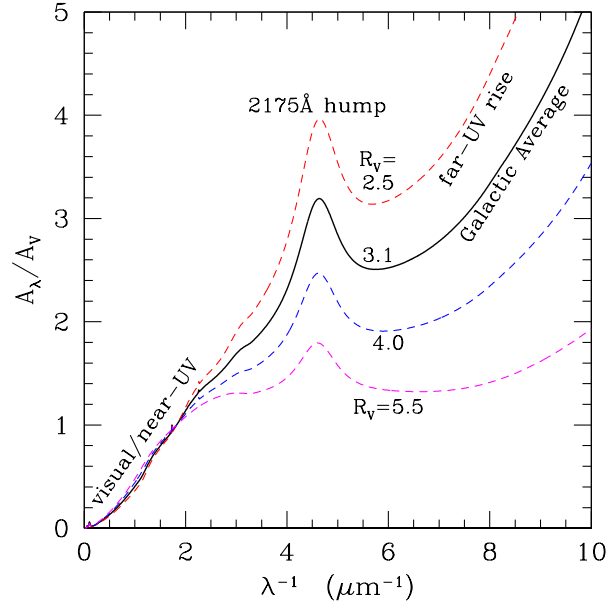

Fig. 1 Interstellar extinction curves of the Milky Way ($R_V = 2.5$, 3.1, 4.0, 5.5). There exist considerable regional variations in the Galactic optical UV extinction curves, as characterized by the total-to-selective extinction ratio R_V, indicating that dust grains on different sightlines have different size distributions.

2 The Milky Way

2.1 UV/Optical Extinction: Strong Dependence on Environments

The interstellar extinction curve is usually expressed as A_λ/A_V, where A_V is the extinction in the V band. This means of expressing the extinction curve is not unique; it has also been a common practice to use instead the ratios of two colors, $E(\lambda - V)/E(B - V)$, where $E(\lambda - V) \equiv A_\lambda - A_V$, and A_B is the extinction in the blue (B) band. The Galactic interstellar extinction curves have now been measured for a large number of sightlines over a wide wavelength range ($0.1\,\mu m < \lambda < 20\,\mu m$). As shown in Figure 1, the extinction curves plotted against the inverse wavelength λ^{-1} rise almost linearly from the near-IR to the near-UV, with a broad absorption bump

at about $\lambda^{-1} \approx 4.6\,\mu\mathrm{m}^{-1}$ ($\lambda \approx 2175\,\text{Å}$) and followed by a steep rise into the far-UV at $\lambda^{-1} \approx 10\,\mu\mathrm{m}^{-1}$, the shortest wavelength at which the extinction has been measured. Note the extinction curve does not show any sign of a turnover in the far-UV rise.

The Galactic extinction curves are known to vary significantly among sightlines in the UV/optical at $\lambda < 0.7\,\mu\mathrm{m}$, including strong and weak 2175 Å bumps, and steep and flat far-UV extinction (see Figure 1). Cardelli et al. (1989) found that the variation in the UV/optical can be characterized as a one-parameter function (hereafter "CCM") of $R_V \equiv A_V/E(B-V)$, the optical total-to-selective extinction ratio. The value of R_V depends upon the environment along the line of sight. Low-density regions usually have a rather low value of R_V, having a strong 2175 Å bump and a steep far-UV rise at $\lambda^{-1} > 4\,\mu\mathrm{m}^{-1}$. Lines of sight penetrating into dense clouds, such as the Ophiuchus or Taurus molecular clouds, usually have $4 < R_V < 6$, showing a weak 2175 Å bump, and a relatively flat far-UV rise. The "average" extinction law for the Galactic diffuse interstellar medium (ISM) is described by a CCM extinction curve with $R_V \approx 3.1$, which is commonly used to correct observations for dust extinction. Theoretically, R_V may become infinity in dense regions rich in very large, "gray" grains (i.e., the extinction caused by these grains does not vary much with wavelength), while the steep extinction produced completely by Rayleigh scattering would have $R_V \sim 0.72$ (Draine 2003). A wide range of R_V values have been reported for extragalactic lines of sight, ranging from $R_V \approx 0.7$ for a quasar intervening system at $z \approx 1.4$ (Wang et al. 2004) to $R_V \approx 7$ for gravitational lensing galaxies (Falco et al. 1999). However, the one-parameter CCM formula of R_V does not apply to sightlines beyond the MW (see Clayton 2004).

The exact nature of the carrier of the 2175 Å extinction bump remains unknown since its first discovery nearly half a century ago (Stecher 1965). Recently, a popular hypothesis is that it is due to the $\pi - \pi^*$ transition of polycyclic aromatic hydrocarbon (PAH) molecules (Joblin et al. 1992, Li & Draine 2001, Cecchi-Pestellini et al. 2008, Malloci et al. 2008, Steglich et al. 2010, Mulas et al. 2013).

2.2 Near-IR Extinction: A Universal Power Law?

With the wealth of available data from space-borne telescopes (e.g., *ISO* and *Spitzer*) and ground-based surveys (e.g., *2MASS*) in the near- and mid-IR, in recent years we have seen an increase in interest in IR extinction. Understanding the effects of dust extinction in the IR wavelengths is important to properly interpret these observations.

As the UV/optical extinction varies substantially among various environments, one might expect the near-IR extinction at $0.9\,\mu\mathrm{m} < \lambda < 3\,\mu\mathrm{m}$ to vary correspondingly. However, for over two decades astronomers have believed that there is little, if any, near-IR extinction variation from one line of sight to another. The near-IR extinction law appears to be an approximately uniform power law of $A_\lambda \sim \lambda^{-\alpha}$ with $\alpha \approx 1.6$–1.8, independent of environment or R_V at $0.9\,\mu\mathrm{m} < \lambda < 3\,\mu\mathrm{m}$. Martin & Whittet (1990) found $\alpha \approx 1.8$ in the diffuse ISM as well as the outer regions of
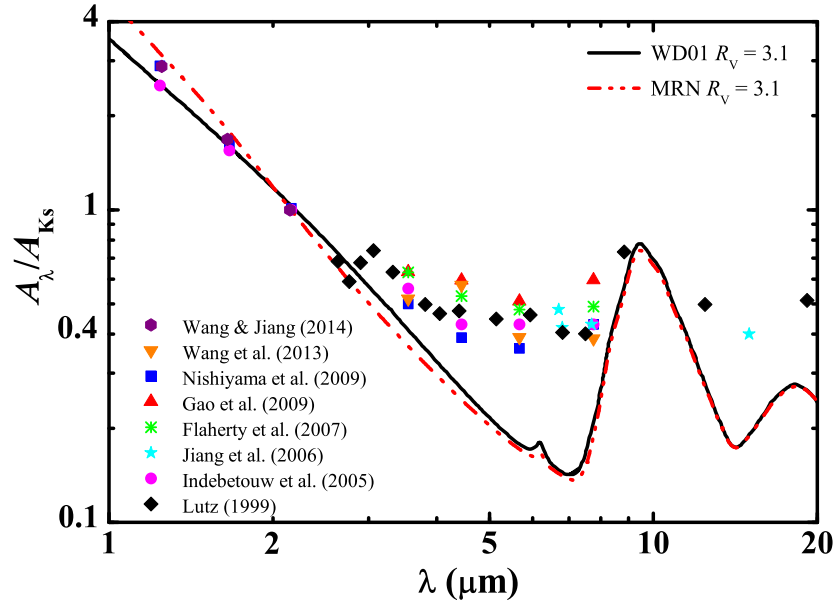
Fig. 2 Comparison of the IR extinction observed for various interstellar regions with that predicted from the MRN (dot-dashed line) and WD01 (solid line) silicate-graphite models for the diffuse ISM of which the UV/optical extinction is characterized by $R_V \approx 3.1$. The little bump at $6.2\,\mu$m arises from the C–C stretching absorption band of PAHs (see Li & Draine 2001).

the ρ Oph and Tr 14/16 clouds. Using a large sample of obscured OB stars, He et al. (1995) found that the near-IR extinction can be well-fitted to a power law with $\alpha \approx 1.73 \pm 0.04$, even though R_V varies between 2.6 and 4.6. A "universal" power law also well describes the near-IR polarization P_λ which, like the near-IR extinction, probes the large, submicron-sized grain population, $P_\lambda/P_{max} \propto \lambda^{-1.8}$, where P_{max} is the peak polarization (Martin & Whittet 1990).

However, much steeper power-laws have also been derived for the near-IR extinction. Stead & Hoare (2009) determined $\alpha \approx 2.14^{+0.04}_{-0.05}$ for the slope of the near-IR extinction power law for eight regions of the MW between $l \sim 27^{\rm o}$ and $\sim 100^{\rm o}$. Nishiyama et al. (2009) explored the extinction law toward the Galactic center. They derived the index of the power law $\alpha \approx 1.99$. Fritz et al. (2011) found $\alpha \approx 2.11$ for the Galactic center extinction.

Based on a spectroscopic study of the 1–$2.2\,\mu$m extinction law toward a set of nine ultracompact HII regions with $A_V > 15$ mag, Moore et al. (2005) found some evidence that the near-IR extinction curve may tend to flatten at higher extinction. They argued that flatter curves are most likely the result of increasing the upper limit of the grain-size distribution in regions of higher extinction. Naoi et al. (2006) determined the near-IR color excess ratio $E(\mathrm{J}-\mathrm{H})/E(\mathrm{H}-\mathrm{K_S})$, one of the simplest

parameters for expressing the near-IR extinction law, for L1688, L1689, and L1712 in the ρ Oph cloud, and Cha I, Cha II, and Cha III in the Chamaeleon cloud. They found that $E(\mathrm{J-H})/E(\mathrm{H-K_S})$ changes with increasing optical depth, consistent with grain growth toward the inside of the dark clouds.

More recently, Wang & Jiang (2014) examined the apparent colors of 5,942 K-type giants whose intrinsic J, H, $\mathrm{K_S}$ colors are known from their effective stellar temperatures determined from the SDSS-III APOGEE survey. They derived a nearly constant near-IR color excess ratio of $E(\mathrm{J-H})/E(\mathrm{H-K_S}) \approx 0.64$ (which corresponds to $\alpha \approx 1.95$), independent of the amount of extinction in the color excess range of $0.3 < E(\mathrm{J-K_S}) < 4.0$.

A "universal" near-IR extinction law of a constant power-index α for regions with different physical conditions is difficult to understand. One would imagine that in denser regions the dust could be larger which would lead to a smaller α. However, this tendency is not observationally verified (see Figure 7 of Wang et al. 2013).
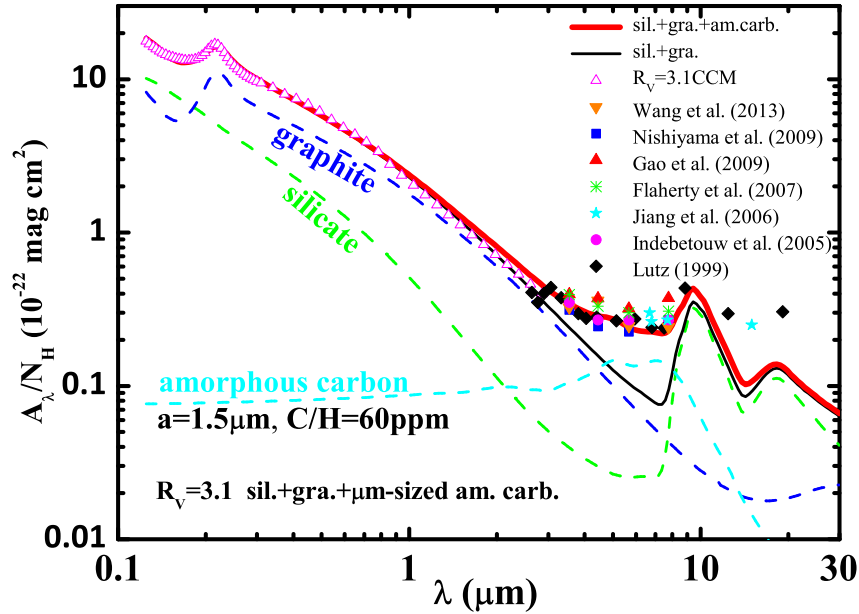

Fig. 3 Fitting the $R_V = 3.1$ UV/optical, near- and mid-IR extinction with a simple mixture (dot-dashed line) of amorphous silicate (dotted line) and graphite dust (dashed line), together with a population of large, μm-sized amorphous carbon of spherical radii $a \approx 1.5\,\mu$m and C/H ≈ 60 ppm (Wang, Li & Jiang 2014). The thick solid line plots the model fit, while the symbols plot the observed extinction: the open pentagons plot the $R_V = 3.1$ UV/optical/near-IR extinction, and the other symbols plot the mid-IR extinction.

2.3 Mid-IR Extinction: Universally Flat?

The mid-IR extinction at $3\,\mu$m $< \lambda < 8\,\mu$m (in between the power-law regime at $\sim$1–3 μm and the $9.7\,\mu$m silicate Si–O stretching absorption feature) is not well understood. The determination of the mid-IR extinction law has been more difficult because this wavelength range is best accessed from space. All dust models for the diffuse ISM predict an extinction curve steeply declines with λ at $1\,\mu$m $< \lambda < 7\,\mu$m (at $\lambda > 7\,\mu$m, the extinction increases because of the $9.7\,\mu$m silicate absorption band). As shown in Figure 2, the Weingartner & Draine (2001b; WD01) silicate-graphite grain model predicts a power-law of $A_\lambda \propto \lambda^{-1.74}$ for the IR extinction at $1\,\mu$m $< \lambda < 7\,\mu$m, while the Mathis, Rumpl, & Nordsieck (1977; MRN) model predicts a steeper power-law of $A_\lambda \propto \lambda^{-2.02}$. The model IR extinction curves reach their minimum at $\sim7\,\mu$m where the extinction power-law intersects the blue-wing of the $9.7\,\mu$m silicate absorption band.

Rieke & Lebofsky (1985) measured the IR extinction from $1\,\mu$m to $13\,\mu$m for the lines of sight toward o Sco, a normal A5 II star behind the edge of the ρ Oph cloud obscured by $A_V \approx 2.92\,$mag, and toward a number of stars in the Galactic center. They derived a power-law of $A_\lambda \propto \lambda^{-1.62}$ for $1\,\mu$m $< \lambda < 7\,\mu$m for o Sco and the Galactic center sources. Draine (1989) compiled the IR extinction observed for a range of Galactic regions including diffuse clouds, molecular clouds, and HII regions. A power-law of $A_\lambda \propto \lambda^{-1.75}$ for $1\,\mu$m $< \lambda < 7\,\mu$m was obtained. Bertoldi et al. (1999) and Rosenthal et al. (2000) also derived a power-law extinction of $A_\lambda \propto \lambda^{-1.7}$ for $2\,\mu$m $< \lambda < 7\,\mu$m for the Orion molecular cloud (OMC) which displays an absorption band at $3.05\,\mu$m attributed to water ice.

However, numerous recent observations suggest that the mid-IR extinction at $3\,\mu$m $< \lambda < 8\,\mu$m appears to be almost *universally* flat or "gray" for both diffuse and dense environments, much flatter than that predicted from the MRN or WD01 silicate-graphite model for $R_V = 3.1$ (see Figure 2).

Lutz et al. (1996) derived the extinction toward the Galactic center star Sgr A* between $2.5\,\mu$m and $9\,\mu$m from the H recombination lines. They found that the Galatic center extinction shows a flattening of A_λ in the wavelength region of $3\,\mu$m $< \lambda < 9\,\mu$m, clearly lacking the pronounced dip at $\sim7\,\mu$m predicted from the $R_V = 3.1$ silicate-graphite model (see Figure 2). This was later confirmed by Lutz (1999), Nishiyama et al. (2009), and Fritz et al. (2011).

Indebetouw et al. (2005) used the photometric data from the *2MASS* survey and the *Spitzer*/GLIMPSE Legacy program to determine the IR extinction. From the color excesses of background stars, they derived the $\sim$1.25–8 μm extinction laws for two very different lines of sight in the Galactic plane: the $l = 42^{\rm o}$ sightline toward a relatively quiescent region, and the $l = 284^{\rm o}$ sightline which crosses the Carina Arm and contains RCW 49, a massive star-forming region. The extinction laws derived for these two distinct Galactic plane fields are remarkably similar: both show a flattening across the 3–8 μm wavelength range, consistent with that derived by Lutz et al. (1996) for the Galactic center.

Jiang et al. (2006) derived the extinction at 7 and $15\,\mu$m for more than 120 sight-lines in the inner Galactic plane based on the ISOGAL survey data and the near-IR

data from DENIS and 2MASS, using RGB tip stars or early AGB stars (which have only moderate mass loss) as the extinction tracers. They found the extinction well exceeding that predicted from the MRN or WD01 $R_V = 3.1$ models.

Flaherty et al. (2007) obtained the mid-IR extinction laws in the *Spitzer*/IRAC bands for five nearby star-forming regions. The derived extinction laws at $\sim$4–8 μm are flat, even flatter than that of Indebetouw et al. (2005).

Gao, Jiang, & Li (2009) used the *2MASS* and *Spitzer*/GLIPMSE data to derive the extinction in the four IRAC bands for 131 GLIPMSE fields along the Galactic plane within $|l| \leq 65^{\circ}$ (Benjamin et al. 2003, Churchwell et al. 2006). Using red giants and red clump giants as the extinction tracers, they also found the mean extinction in the IRAC bands to be flat.

Wang et al. (2013) determined the mid-IR extinction in the four *Spitzer*/IRAC bands of five individual regions in Coalsack, a nearby starless dark cloud, spanning a wide variety of interstellar environments from diffuse and translucent to dense clouds. They found that all regions exhibit a flat mid-IR extinction.

All these observations appear to suggest an "universally" flat extinction law in the mid-IR, with little dependence on environments. Draine (2003) extended the WD01 model of $R_V = 5.5$ into the IR up to $\lambda < 30 \mu$m and found that the WD01 $R_V = 5.5$ model closely reproduces the flat mid-IR extinction observed toward the Galactic center (Lutz et al. 1996). Dwek (2004) hypothesized that the observed mid-IR extinction is largely due to metallic needles for which the opacity is high in the mid-IR. Wang, Li, & Jiang (2014) found that the mid-IR extinction as well as the UV/optical extinction could be closely reproduced by a mixture of submicron-sized amorphous silicate and graphite, and a population of micrometer-sized amorphous carbon which consumes $\sim$60 carbon atoms per million (ppm) hydrogen atoms (see Figure 3).

2.4 IR Extinction as a Probe of the Galactic Structure

Whittet (1977) presented observational evidence for a small but appreciable variation in R_V with Galactic longitude. He suggested that the most likely explanation for this is a variation in the mean size of the dust in the local spiral arm. However, unfortunately only a few data points were used in that work and therefore no systematic variation of the extinction with Galactic longitude was reported. A major leap forward occurred recently thanks to the amazing success of the *Spitzer*/GLIMPSE Legacy programs (see Benjamin 2014).

Based on the IR extinction in the four IRAC bands derived for 131 GLIMPSE fields in the Galactic plane, Gao, Jiang, & Li (2009) demonstrated that the mid-IR extinction appears to vary with Galactic longitude; more specifically, the locations of the spiral arms seem to coincide with the dips of the extinction ratios A_{λ}/A_{K_S} (see Figure 4). In particular, the coincidence of the locations of the A_{λ}/A_{K_S} minimum and the spiral arms is outstanding at negative longitudes (e.g., the Crux-Scutum arm at $l = -50^{\circ}$, the Norma arm at -33°, and the southern tangent of the 3 kpc
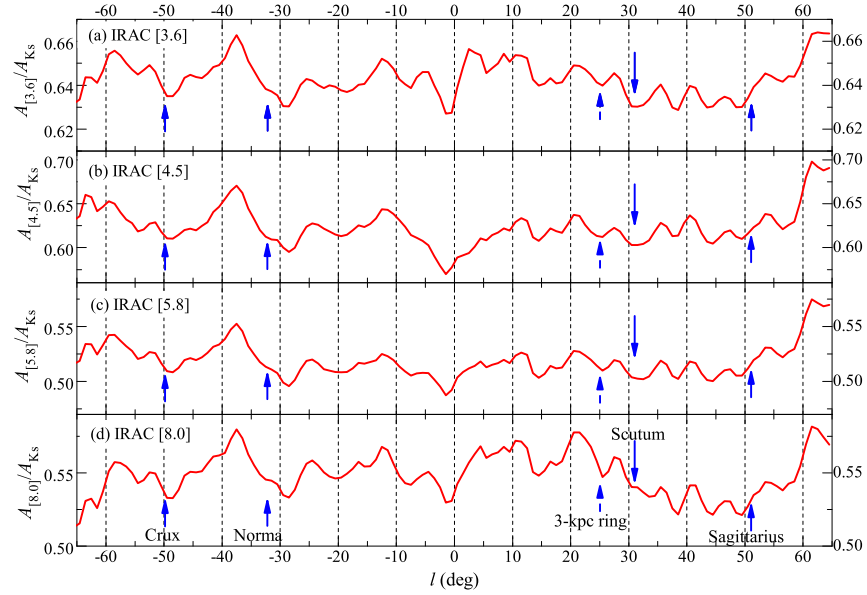
Fig. 4 Longitudinal distributions of A_λ/A_{K_S} in the four IRAC bands (solid lines; Gao, Jiang & Li 2009). The dips of the extinction ratios A_λ/A_{K_S} appear to coincide with the locations of the spiral arms. The solid vertical arrows show the tangent directions of the spiral arms at $l = -50°, -33°, 31°$ and $51°$ (Vallée 2008). The dashed arrow shows the tangent direction of the 3 kpc ring at $l = 23°$ (Dame & Thaddeus 2008).

ring around $-23°$). For the positive longitudes, the locations of the Scutum-Crux arm and the Sagittarius-Carina arm also coincide with the valleys of A_λ/A_{K_S}. For the broad dip around $l = 16°$, there is no clear tangent direction to any arms, but this direction points to the start of the Norma arm and the Scutum-Crux arm (see Figure 2 of Vallée 2008), and probably one end of the Galactic bar.

Using data from *2MASS* and *Spitzer*/IRAC for G and K spectral type red clump giants, Zasowski et al. (2009) also found longitudinal variations of the 1.2–8 μm IR extinction over $\sim$150° of contiguous Galactic mid-plane longitude; more specifically, they found strong, monotonic variations in the extinction law shape as a function of angle from the Galactic center, symmetric on either side of it: the IR extinction law becomes increasingly steep as the Galactocentric angle increases, with identical behavior between $l < 180°$ and $l > 180°$ (see Figure 5).
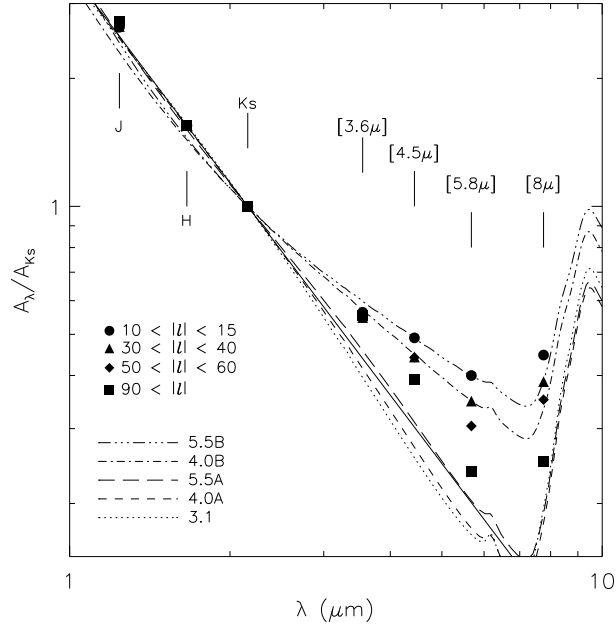
Fig. 5 Mean extinction curves for the indicated ranges of Galactic angle (circles: $10° < |l| < 15°$; triangles: $30° < |l| < 40°$; diamonds: $50° < |l| < 60°$; squares: $|l| > 90°$), compared to that of the WD01 model for $R_V = 3.1, 4.0, 5.5$. Also shown for comparison is an $A_\lambda \propto \lambda^{-\beta}$ power law, with $\beta = 1.66$ (solid line). It is apparent that the extinction curve becomes increasingly steep at larger Galactocentric angles (Zasowski et al. 2009).

3 SMC

As our nearest galactic neighbors, the Magellanic Clouds offer a unique opportunity to study the effects of different galactic environments on dust properties. As a metal-poor (with a metallicity only $\sim 1/10$ of that in the MW; see Kurt & Dufour 1998) and gas-rich (with a dust-to-gas ratio over 10 times lower than in the MW; see Bouchet et al. 1985) irregular dwarf galaxy, the SMC is often considered as a local analog of primordial galaxies at high redshifts which must have formed at very low metallicity. Therefore, the dust in the SMC which differs substantially from that in the MW allows us to probe the primordial conditions in more distant galaxies. Indeed, the SMC-type extinction often provides better fits to the spectral energy distributions (SEDs) of many extragalactic systems than the "standard" MW-type extinction curve (e.g., see Richards et al. 2003 and Hopkins et al. 2004 for reddened quasars, and Vijh et al. 2003 for Lyman break galaxies). The 2175 Å feature seen in the MW-type extinction is absent in the attenuation curve inferred from radiative transfer modeling of starburst galaxies including stars, gas and dust (Calzetti et al. 1994, Gordon et al. 1997).
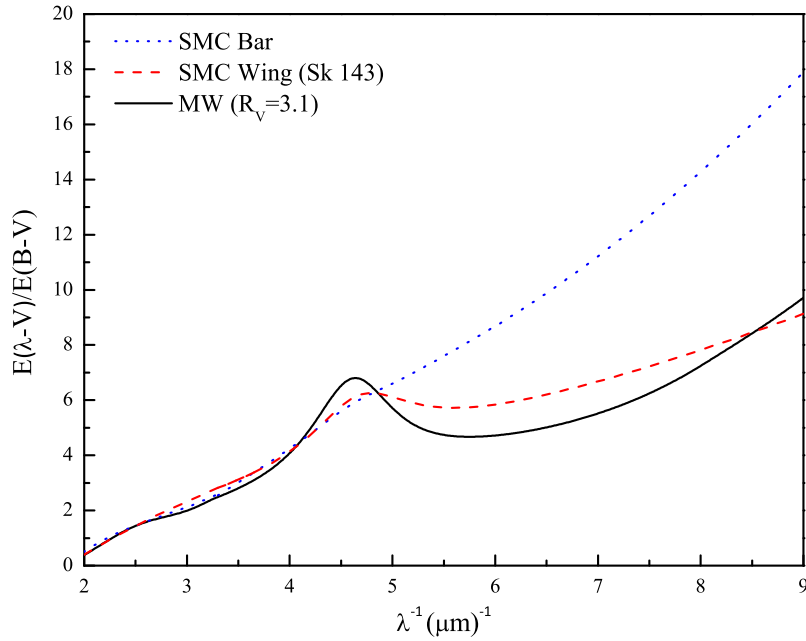
Fig. 6 Comparison of the SMC Bar (dotted) and MW $R_V = 3.1$ (solid) extinction curves. Also shown is the extinction curve for the sightline toward the SMC wing star Sk 143 (dashed).

Due to its low metallicity, the dust quantity (relative to H) in the SMC is expected to be lower than that of the MW because there is less raw material (i.e., heavy elements) available for making the dust. The (relative) lack of the dust-making raw material could prevent the dust in the SMC from growing and hence the dust in the SMC may be smaller than the MW dust. Furthermore, the star-formation activity in the SMC could destroy the dust. Therefore, one would naturally expect the dust size distribution and extinction curve in the SMC to differ from that of the MW.

There are significant regional variations in the UV/optical extinction properties of the SMC. As shown in Figure 6, the extinction curve of the SMC Bar displays a nearly linear rise with λ^{-1} and no detectable 2175 Å extinction bump (Lequeux et al. 1982; Cartledge et al. 2005), presumably due to the destruction of the carriers of the 2175 Å hump by the intense UV radiation and shocks associated with star formation. In contrast, the extinction curve for the line of sight toward Sk 143 (AvZ 456) has a strong 2175 Å hump (Lequeux et al. 1982; Cartledge et al. 2005). This sightline passes through the SMC wing, a region with much weaker star formation (Gordon & Clayton 1998).

The overall IR emission spectrum of the SMC peaks at $\lambda \sim 100\,\mu$m with a local minimum at $\lambda \sim 12\,\mu$m which is commonly believed to be emitted by PAHs (see

Li & Draine 2002). The PAH emission features have been detected locally in the SMC B1#1 quiescent molecular cloud (Reach et al. 2000), and in some star-forming regions (Contursi et al. 2000, Sanstrom et al. 2012). Based on the observed PAH emission and attributing the 2175 Å extinction bump to PAHs, Li & Draine (2002) predicted an extinction excess of $\Delta A_{2175} \approx 0.5$ mag at 2175 Å for sightlines through SMC B1#1. Maíz Apellániz & Rubio (2012) measured the UV extinction for four stars in the SMC B1#1 cloud from their HST/STIS slitless UV spectra. They found that the 2175 Å bump is moderately strong in one star, weak in two stars, and absent in the fourth star.
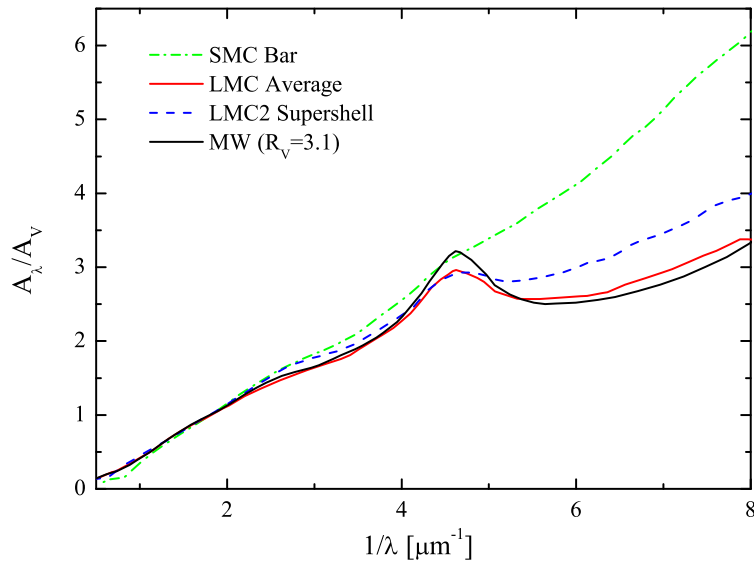

Fig. 7 Comparison of the "LMC Average" (dashed), SMC (dotted), and MW $R_V = 3.1$ (solid) extinction curves. Also shown is the LMC2 supershell extinction curve (dot-dashed). The "LMC Average" curve (also known as the "LMC" curve) is the mean extinction curve derived for the sightlines toward the stars outside of the 30 Dor star-forming region, while the LMC2 supershell curve (also known as the "LMC2" curve or the "LMC 30 Dor" curve) is for the dust inside the LMC2 supergiant shell which, lying on the southeast side of 30 Dor, was formed by the combined stellar winds and supernova explosions from the stellar association at its center.

4 LMC

Like the SMC, the LMC is also a low-metalicity irregular dwarf galaxy and a satellite of the MW. Since the metallicity of the LMC (which is only $\sim$1/4 of that of the MW; Russell & Dopita 1992) is similar to that of galaxies at red shifts $z \sim 1$ (see Dobashi et al. 2008), it offers opportunities to study the dust properties in distant low-metallicity extragalactic environments by studying the extinction properties of the LMC.

As illustrated in Figure 7, the LMC extinction curve is intermediate between that of the MW and that of the SMC: compared to the Galactic extinction curve, the LMC extinction curve is characterized by a *weaker* 2175 Å hump and a *stronger* far-UV rise (Nandy 1981, Koornneef & Code 1981, Gordon et al. 2003). Strong regional variations in extinction properties have also been found in the LMC (Clayton & Martin 1985; Fitzpatrick 1985, 1986; Misselt et al. 1999; Gordon et al. 2003): the sightlines toward the stars inside or near the supergiant shell, LMC 2, which lies on the southeast side of the 30 Doradus star-forming region, have a weak 2175 Å hump (Misselt et al. 1999), while the extinction curves for the sightlines toward the stars which are > 500 pc away from the 30 Doradus region are closer to the Galactic extinction curve.

Based on the photometric data from the *Spitzer*/SAGE survey and with red giants as the extinction tracer, Gao et al. (2013) derived the mid-IR extinction for a number of regions of the LMC in the four IRAC bands. The average mid-IR extinction shows a flat curve, close to the MW $R_V = 5.5$ model extinction curve (see Figure 8).

In the 30 Dor star-forming region where large amounts of UV radiation and shocks are present, the dust is expected to be processed and its size distribution is expected to be modified. The difference between the UV extinction characteristic of the 30 Dor region and that outside the 30 Dor region could be understood in terms of dust erosion in the 30 Dor region which produces a dust size distribution skewed toward smaller grains, and leads to a steeper far-UV extinction and a weaker 2175 Å bump as the bump carriers could also be destroyed.

However, it is difficult to quantify the effects of star-formation activities on the dust size distribution and the corresponding UV extinction. Although the environment of the SMC Bar is likely to be less severe than for the 30 Dor region (which is a much larger star-forming region than any in the SMC), the UV extinction of the SMC Bar is more extreme than that of the LMC 30 Dor, with the former exhibiting a very steep far-UV rise and lacking the 2175 Å bump. The SMC has star formation occurring at only $\sim$1% of the rate of a starburst galaxy. But starburst galaxies appear to be dominated by large, submicron- or micron-sized dust and are characterized by a flat or "gray" extinction curve (see Calzetti 2001). Therefore, many factors including densities, metallicities, and star formation rates must be important in controlling the formation and destruction processes (such as shattering and coagulation) of dust (see Clayton 2004).
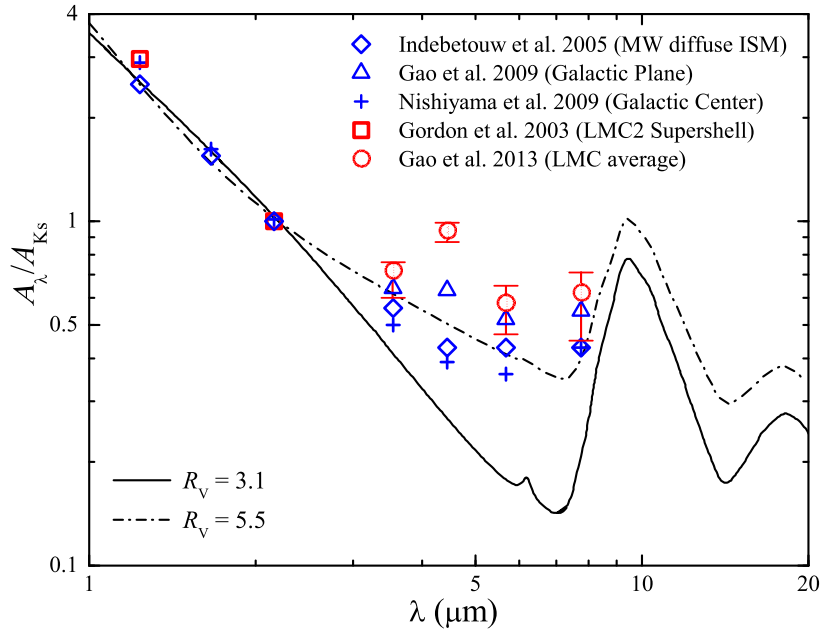
Fig. 8 IR extinction of the LMC compared with the WD01 model curves of $R_V = 3.1$ (solid line) and $R_V = 5.5$ (dot-dashed line). Open squares: the LMC near-IR extinction of Gordon et al. (2003). Filled stars: the mid-IR extinction at the four IRAC bands derived by Gao et al. (2013). Open diamonds: the near- and mid-IR extinction for the MW diffuse ISM of Indebetouw et al. (2005). Open triangles: the average extinction at the four IRAC bands derived from 131 GLIMPSE fields along the Galactic plane (Gao et al. 2009). Pluses: the near- and mid-IR extinction toward the Galactic center of Nishiyama et al. (2009).

5 M 31

The Andromeda galaxy (M 31), at a distance of $\sim$780 kpc (McConnachie et al. 2005), is the only galaxy (other than the MW, and the SMC/LMC) of which individual stars can be resolved and adopted for extinction determination in terms of the "pair method". Unlike the Magellanic Clouds which are metal-poor, M 31 has a super-solar metallicity.

Bianchi et al. (1996) obtained the UV spectra in the $\sim$1150–3300 Å wavelength range of several bright OB stars in M 31, using the *Faint Object Spectrograph* (FOS) on board the *Hubble Space Telescope* (HST). The UV extinction was derived for three sightlines in M 31 and seems to show a MW-type extinction curve but with the 2175 Å feature possibly somewhat weaker than in the MW (see Figure 9).
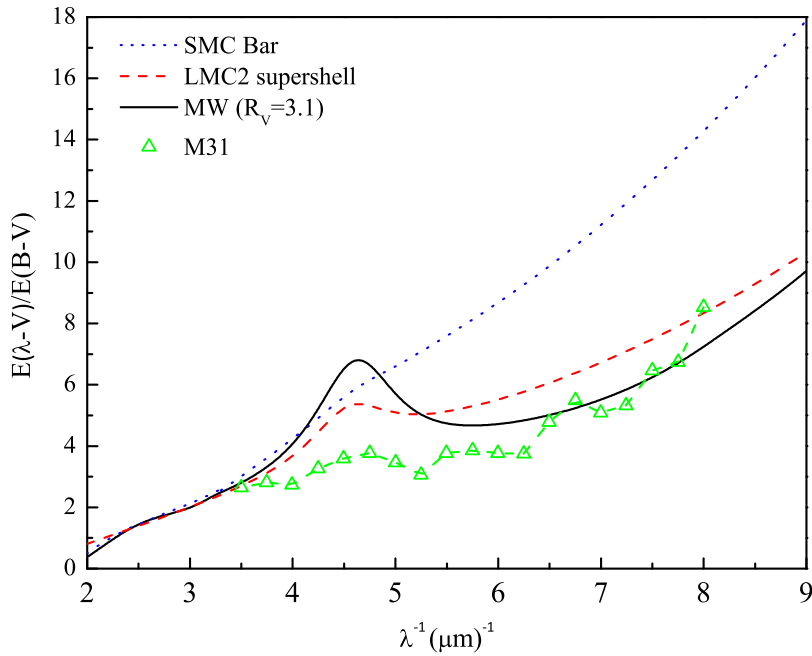
Fig. 9 Comparison of the M 31 (dot-dashed line-connected triangles), MW $R_V = 3.1$ (solid), SMC Bar (dotted), and LMC2 30 Dor "supershell' region (dashed) extinction curves. The M 31 extinction curve was obtained by Bianchi et al. (1996) with the "pair method" by comparing the HST/FOS spectra of reddened M 31 stars and that of unredded Galactic stars of the same spectral type. The M 31 extinction curve has an overall wavelength dependence similar to that of the average Galactic extinction curve but possibly has a weaker 2175 Å bump.

More recently, Dong et al. (2014) measured the extinction curve for the dust in the central $\sim 1'$ (~ 200 pc) region of M 31 at thirteen bands from the mid-UV to near-IR in the wavelength range of ~ 1928 Å–1.5 μm. They examined five representative dusty clumps located in the circumnuclear region, utilizing data from the HST *Wide Field Camera 3* (WFC3) and *Advanced Camera for Surveys* (ACS) detectors as well as the *UV and Optical Telescope* (UVOT) on board *Swift*. They found that the extinction curves of these clumps, with $R_V \approx 2.4$–2.5, are steeper than the average Galactic one, indicating that the dust in M 31 is smaller than that in the MW. Dong et al. (2014) also found that one dusty clump (size <2 pc) exhibits a strong 2175 Å bump. They speculated that large, submicron-sized dust in M 31 may have been destroyed in the harsh environments of the bulges by supernova explosions or past activities of the central super-massive black hole, resulting in the observed steepened extinction curve.
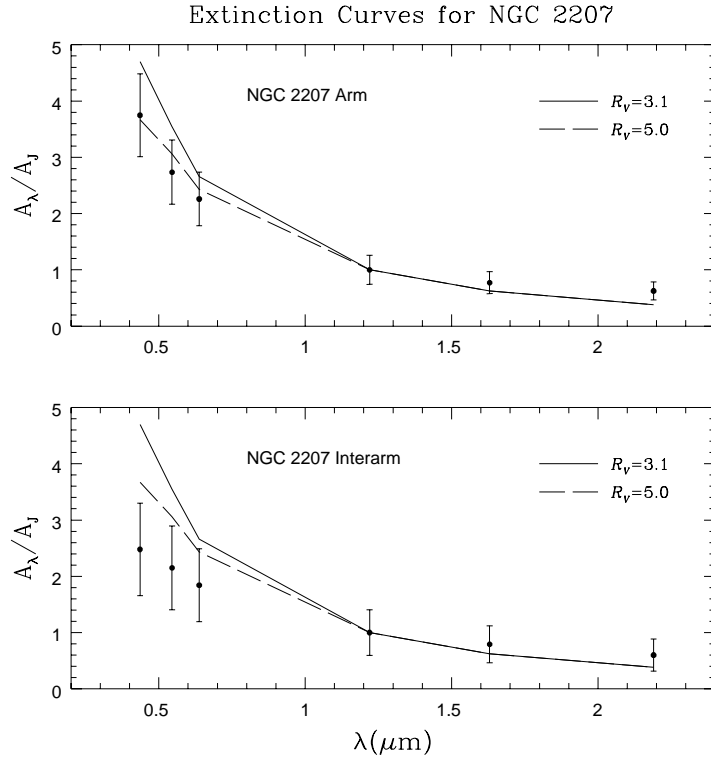
Fig. 10 Extinction curves in the *BVRJHK* bands (normalized to the *J*-band extinction) for the dust in the spiral arm (top) and interarm (bottom) regions of NGC 2207, a spiral galaxy partially occulting the background spiral IC 2163 (Berlind et al. 1997). The solid and dashed lines plot the MW extinction curves for $R_V = 3.1$ and $R_V = 5.0$, respectively. Note that the extinction curves in both the spiral arm and interarm regions of NGC 2207 are flatter ("grayer") than the MW average of $R_V = 3.1$, while the interarm extinction curve is even "grayer" than that of the spiral arm.

6 Dust in Galaxies beyond the Local Group

The CCM extinction relation is applicable to a wide range of interstellar dust environments in the MW, including lines of sight through diffuse dust and dark cloud dust, as well as dust associated with star formation. However, the CCM relation does not appear to apply beyond the MW even in other Local Group galaxies such as the Magellanic Clouds and M 31 (see Clayton 2004). Unfortunately, high signal-to-noise extinction curves are still available for only three galaxies, the MW, LMC, and SMC. Direct measurements of extragalactic UV extinction using individual reddened stellar sightlines are still limited to the LMC, SMC and a few sightlines in M 31 (see §5). As summarized by Draine (2003), there are several different approaches to determining the extinction curve for dust in galaxies where individual stars cannot be resolved.

White & Keel (1992) proposed that the dust extinction curve of an external galaxy can be determined directly if it lies in front of another galaxy. The ideal case consists of a face-on symmetric spiral galaxy half overlapping with a symmetric, background spiral or elliptical galaxy. The galaxies need to be symmetric so that their non-overlapping parts may be used to estimate the surface brightness of their overlapping parts. This method has been applied to a number of overlapping galaxy pairs (White & Keel 1992; White et al. 1996, 2000; Keel & White 2001a,b).

Using this technique, Berlind et al. (1997) measured the extinction curves in the $BVRJHK$ visual to near-IR wavelength range for the dust in the spiral arm and interarm regions of NGC 2207 which overlaps IC 2163. This pair consists of two symmetric, almost face-on interacting spiral galaxies which are partially overlapping. These galaxies have been observed and modeled in detail by D. Elmegreen et al. (1995) and B. Elmegreen et al. (1995).

Berlind et al. (1997) found that the dust in NGC 2207 is mainly concentrated in its spiral arms, leaving its interarm regions mostly transparent. More interestingly, they found that the extinction curve in the spiral arm region of NGC 2207 is flat, resembling the MW extinction curve for $R_V \approx 5.0$, while the interarm dust appears to be even "grayer" (see Figure 10). They proposed that an unresolved patchy dust distribution in NGC 2207 could be capable of producing the observed extinction curves; and the arm-interarm difference in the observed extinction could also be explained if the interarm region has a higher degree of dust patchiness (i.e., a larger density ratio between the high-density and low-density phases) than the arm region.

Finally, we note that there are some distant extragalactic point sources that can be used to construct extinction curves if their intrinsic SEDs are well characterized. These include QSOs and gamma-ray bursts (GRBs).

By comparing the composite spectra of unreddened and reddened quasars (Vanden Berk et al. 2001), one can derive the extinction curve for quasar sightlines. Richards et al. (2003) and Hopkins et al. (2004) found that the reddening toward thousands of SDSS quasars is dominated by SMC-type dust, but some studies argue for "gray" dust (see Li 2007).

Distant quasars have also been used as a background source to determine the dust extinction of damped Lyα absorption systems (e.g., see Wang et al. 2012) and intervening (e.g., Mg II) absorption systems (e.g., see Wang et al. 2004, Zhou et al. 2010, Jiang et al. 2010a,b, 2011).

Gravitationally-lensed quasars with multiple images can also be used to determine the extinction curves of distant galaxies (e.g., see Motta et al. 2002, but also see McGough et al. 2005).

GRBs, owing to their intense luminosity (emitting up to $\sim 10^{53}$ erg), allow their detection up to very high redshifts. Particularly, the featureless, power law-like spectral shapes of their afterglows, make GRBs an excellent probe of the dust extinction for the GRB host galaxies (e.g., see Li et al. 2008, Liang & Li 2009, 2010).

We note that the 2175 Å extinction bump has been detected in both nearby and distant galaxies (see Xiang, Li, & Zhong 2011 and references therein).

References

1. Ascenso, J., Lada, C. J., Alves, J., Román-Zúñiga, C. G., & Lombardi, M. 2013, A&A, 549, A135
2. Benjamin, R. A., et al. 2003, PASP, 115, 953
3. Benjamin, R.A. 2014, in Lessons from the Local Group – A Conference in Honour of David Block and Bruce Elmegreen, ed. K.C. Freeman, B.G. Elmegreen, D.L. Block, & M. Woolway (Springer: New York), in press
4. Berlind, A. A., Quillen, A. C., Pogge, R. W., & Sellgren, K. 1997, AJ, 114, 107
5. Bertoldi, F., Timmermann, R., Rosenthal, D., Dropatz, S., et al. 1999, A&A, 346, 267
6. Bianchi, L., Clayton, G. C., Bohlin, R. C., Hutchings, J. B., & Massey, P. 1996, ApJ, 471, 203
7. Bless, R. C., & Savage, B. D. 1970, in IAU Symp. 36, Ultraviolet Stellar Spectra and Related Ground-based Observations, ed. L. Houziaux & H. E. Butler (Dordecht: Reidel), 28
8. Block, D. L. 1996, in New Extragalactic Perspectives in the New South Africa, ed. D. L. Block & J. M. Greenberg (Dordrecht: Kluwer), 1
9. Block, D. L., & Wainscoat, R. J. 1991, Nature, 353, 48
10. Block, D. L., & Sauvage, M. 2000, A&A, 353, 72
11. Block, D. L., Elmegreen, B. G., Stockton, A., & Sauvage, M. 1997, ApJ, 486, L95
12. Block, D. L., Bertin, G., Stockton, A., Grosbøl, P., Moorwood, A. F. M., & Peletier, R. F. 1994, A&A, 288, 365
13. Bouchet, P., Lequeux, J., Maurice, E., et al. 1985, A&A, 149, 330
14. Butler, M. J., & Tan, J. C. 2012, ApJ, 754, 5
15. Calzetti, D. 2001, PASP, 113, 1449
16. Calzetti, D., Kinney, A. L., & Storchi-Bergmann, T. 1994, ApJ, 429, 582
17. Cardelli, J. A., Clayton, G. C., & Mathis, J. S. 1989, ApJ, 345, 245
18. Cartledge, S. I. B., Clayton, G. C., Gordon, K. D., et al. 2005, ApJ, 630, 355
19. Cecchi-Pestellini, C., Malloci, G., Mulas, G., et al. 2008, A&A, 486, L25
20. Churchwell, E, Povich, M. S., Allen, D., et al. 2006, ApJ, 649, 759
21. Clayton, G. C., & Martin, P. G. 1985, ApJ, 288, 558
22. Clayton, G. C. 2004, in Astrophysics of Dust (ASP Conf. Ser. 309), ed. A.N. Witt, G.C. Clayton, & B.T. Draine (San Francisco, CA: ASP), 57
23. Contursi, A., Lequeux, J., Cesarsky, D., et al. 2000, A&A, 362, 310
24. Dame, T. M., & Thaddeus, P. 2008, ApJ, 683, L143
25. Davenport, J. R. A., Ivezić, Ž., Becker, A. C., et al. 2014, MNRAS, 440, 3430
26. Dobashi, K., Bernard, J. P. Hughes, A., et al. 2008, A&A, 484, 205
27. Dong, H., Li, Z., Wang, Q. D., et al. 2014, ApJ, 785, 136
28. Draine, B. T. 1989, in Infrared Spectroscopy in Astronomy, ed. B.H. Kaldeich (Paris: ESA Publications Division), 93
29. Draine, B. T. 2003, ARA&A, 41, 241
30. Draine, B.T., & Li, A. 2001, ApJ, 551, 807
31. Draine, B.T., & Li, A. 2007, ApJ, 657, 810
32. Draine, B. T., Dale, D. A., Bendo, G., et al. 2007, ApJ, 663, 866
33. Draine, B. T., Aniano, G., Krause, O., et al. 2014, ApJ, 780, 172

34. Dwek, E., Arendt, R. G., Hauser, M. G., et al. 1998, ApJ, 508, 106
35. Dwek, E. 2004, ApJ, 611, L109
36. Elíasdóttír, Á., et al. 2009, ApJ, 697, 1725
37. Elmegreen, B.G., Sundin, M., Kaufman, M., Brinks, E., & Elmegreen, D.M. 1995, ApJ, 453, 139
38. Elmegreen, D.M., Kaufman, M., Brinks, E., Elmegreen, B.G., & Sundin, M. 1995, ApJ, 453, 100
39. Falco, E. E., Impey, C. D., Kochanek, C. S., et al. 1999, ApJ, 523, 617
40. Fazio, G. G. 2010, in Galaxies and Their Masks, ed. D. L. Block, K. C. Freeman, & I. Puerari (New York: Springer), 425
41. Fitzpatrick, E.L. 1985, ApJ, 299, 219
42. Fitzpatrick, E.L. 1986, AJ, 92, 1068
43. Fitzpatrick, E. L., & Massa, D. 2009, ApJ, 699, 1209
44. Flaherty, K., Pipher, J., Megeath, S., et al. 2007, ApJ, 663, 1069
45. Fritz, T. K., Gillessen, S., et al. 2011, ApJ, 737, 73
46. Galliano, F., Hony, S., Bernard, J.-P., et al. 2011, A&A, 536, A88
47. Gao, J., Jiang, B. W., & Li, A. 2009, ApJ, 707, 89
48. Gao, J., Jiang, B. W., Li, A., & Xue, M.Y. 2013, ApJ, 776, 7
49. Gordon, K. D., & Clayton, G.C. 1998, ApJ, 500, 816
50. Gordon, K. D., Calzetti, D., & Witt, A. N. 1997, ApJ, 487, 625
51. Gordon, K. D., Clayton, G. C., Misselt, K. A., et al. 2003, ApJ, 594, 279
52. Gordon, K. D., Meixner, M., Meade, M. R., et al. 2011, AJ, 142, 102
53. Gordon, K. D., Roman-Duval, J., Bot, C., et al. 2014, ApJ, in press
54. Greenberg, J.M. 1968, in Stars and Stellar Systems, Vol. VII, ed. B.M. Middlehurst, & L.H. Aller, (Chicago: Univ. of Chicago Press), 221
55. He, L., Whittet, D. C. B., Kilkenny, D., & Spencer Jones, J. H. 1995, ApJS, 101, 335
56. Hensley, B., & Draine, B. T. 2014, AAS, 224, 220.15
57. Hopkins, P. F., Strauss, M. A., Hall, P. B., et al. 2004, AJ, 128, 1112
58. Indebetouw, R., et al. 2005, ApJ, 619, 931
59. Jiang, B. W., Gao, J., Omont, A., Schuller, F., & Simon, G. 2006, A&A, 446, 551
60. Jiang, P., Ge, J., Prochaska, J. X., et al. 2010a, ApJ, 720, 328
61. Jiang, P., Ge, J., Prochaska, J. X., et al. 2010b, ApJ, 724, 1325
62. Jiang, P., Ge, J., Zhou, H., Wang, J., & Wang, T. 2011, ApJ, 732, 110
63. Joblin, C., Leger, A., & Martin, P. 1992, ApJ, 393, L79
64. Jones, A. P., Fanciullo, L., Köhler, M., et al. 2013, A&A, 558, A62
65. Kapteyn, J.C. 1904, ApJ, 24, 115
66. Keel, W. C., & White, R. E., III. 2001a, AJ, 121, 1442
67. Keel, W. C., & White, R. E., III. 2001b, AJ, 122, 1369
68. Koornneef, J., & Code, A. D. 1981, ApJ, 247, 860
69. Kurt, C. M., & Dufour, R. J. 1998, RevMexAA Conf. Ser., 7, 202
70. Lequeux, J., et al. 1982, A&A, 113, L15
71. Li, A. 2004, in Penetrating Bars through Masks of Cosmic Dust, ed. D. L. Block, et al. (New York: Springer), 535
72. Li, A. 2005, J. Phys. Conf. Ser., 6, 229
73. Li, A. 2007, in The Central Engine of Active Galactic Nuclei (ASP Conf. Ser. 373), ed. L. C. Ho & J.-M. Wang (San Francisco, CA: ASP), 561
74. Li, A., & Draine, B.T. 2001, ApJ, 554, 778
75. Li, A., & Draine, B.T. 2002, ApJ, 576, 762
76. Li, A., & Draine, B.T. 2012, ApJ, 760, L35
77. Li, A., & Greenberg, J.M. 1997, A&A, 323, 566
78. Li, A., & Greenberg, J.M. 1998, A&A, 339, 591
79. Li, A., & Mann, I. 2012, in Astrophys. Space Sci. Library, Vol. 385, Nanodust in the Solar System, ed. I. Mann, N. Meyer-Vernet, & A. Czechowski (Springer: Berlin), 5
80. Li, A., Misselt, K. A., & Wang, Y. J. 2006, ApJ, 640, L151
81. Li, A., Liang, S. L., Kann, D. A., et al. 2008, ApJ, 685, 1046

82. Liang, S. L., & Li, A. 2009, ApJ, 690, 56
83. Liang, S. L., & Li, A. 2010, ApJ, 710, 648
84. Lim, W., & Tan, J. C. 2014, ApJ, 780, L29
85. Lutz, D., et al. 1996, ApJ, 315, L269
86. Lutz, D. 1999, in ESA-SP 427, The Universe as Seen by ISO, ed. P. Cox & M. F. Kessler (Noordwijk: ESA), 623
87. Madau, P., & Dickinson, M. 2014, ARA&A, in press (arXiv: 1403.0007)
88. Maíz Apellániz, J., & Rubio, M. 2012, A&A, 541, A54
89. Malloci, G., Mulas, G., Cecchi-Pestellini, C., & Joblin, C. 2008, A&A, 489, 1183
90. Martin, P. G., & Whittet, D. C. B. 1990, ApJ, 357, 113
91. Mathis, J. S., Rumpl, W., & Nordsieck, K. H. 1977, ApJ, 217, 425
92. McConnachie, A. W., Irwin, M. J., Ferguson, A. M. N., et al. 2005, MNRAS, 356, 979
93. McGough, C., Clayton, G. C., Gordon, K. D., & Wolff, M. J. 2005, ApJ, 624, 118
94. Meixner, M., Galliano, F., Hony, S., et al. 2010, A&A, 518, L71
95. Meixner, M., Panuzzo, P., Roman-Duval, J., et al. 2013, AJ, 146, 62
96. Misselt, K. A., Clayton, G. C., & Gordon, K. D. 1999, ApJ, 515, 128
97. Moore, T. J. T., Lumsden, S. L., Ridge, N. A., et al. 2005, MNRAS, 359, 589
98. Motta, V., et al. 2002, ApJ, 574, 719
99. Mulas, G., Zonca, A., Casu, S., & Cecchi-Pestellini, C. 2013, ApJS, 207, 7
100. Nandy, K. Morgan, D. H., Willis, A. J., et al. 1981, MNRAS, 196, 955
101. Naoi, T., Tamura, M., Nakajima, Y., et al. 2006, ApJ, 640, 373
102. Nataf, D. M., Gould, A., Fouqué, P., et al. 2013, ApJ, 769, 88
103. Nishiyama, S., Tamura, M., Hatano, H., et al. 2009, ApJ, 696, 1407
104. Noll, S., et al. 2009, A&A, 499, 69
105. Prochaska, J.X., et al. 2009, ApJ, 691, 27
106. Reach, W. T., Boulanger, F., Contursi, A., & Lequeux, J. 2000, A&A, 361, 895
107. Richards, G. T., Hall, P. B., Vanden Berk, D. E., et al. 2003, AJ, 126, 1131
108. Rieke, G. H., & Lebofsky, M. J. 1985, ApJ, 288, 618
109. Rosenthal, D., Bertoldi, F., & Drapatz, S. 2000, A&A, 356, 705
110. Russell, S. C., & Dopita, M. A. 1992, ApJ, 384, 508
111. Sandstrom, K. M., Bolatto, A. D., Bot, C., et al. 2012, ApJ, 744, 20
112. Stead, J. J., & Hoare, M. G. 2009, MNRAS, 400, 731
113. Stecher, T. P. 1965, ApJ, 142, 1683
114. Steglich, M., Jäger, C., Rouillé, G., et al. 2010, ApJ, 712, l16
115. Struve, F.G.W. 1847, Etudes d'Astronomie Stellaire
116. Valencic, L. A., Clayton, G. C., & Gordon, K. D. 2004, ApJ, 616, 912
117. Vallée, J. P. 2008, ApJ, 681, 303
118. Vanden Berk, D. E., Richards, G. T., Bauer, A., et al. 2001, AJ, 122, 549
119. van der Kruit, P. C. 2014, in Lessons from the Local Group – A Conference in Honour of David Block and Bruce Elmegreen, ed. K.C. Freeman, B.G. Elmegreen, D.L. Block, & M. Woolway (Springer: New York), in press
120. Vijh, U. P., Witt, A. N., & Gordon, K. D. 2003, ApJ, 587, 533
121. Wang, J., Hall, P. B., Ge, J., Li, A., & Schneider, D. P. 2004, ApJ, 609, 589
122. Wang, J.-G., Zhou, H.-Y., Ge, J., et al. 2012, ApJ, 760, 42
123. Wang, S., & Jiang, B.W. 2014, ApJ, 788, L12
124. Wang, S., Li, A., & Jiang, B.W. 2014, Planet. Space Sci., in press
125. Wang, S., Gao, J., Jiang, B.W., Li, A., & Chen, Y. 2013, ApJ, 773, 30
126. Weingartner, J.C., & Draine, B.T. 2001a, ApJS, 134, 263
127. Weingartner, J.C., & Draine, B.T. 2001b, ApJ, 548, 296
128. Whittet, D. C. B. 1977, MNRAS, 180, 29
129. White, R. E., III, & Keel, W. C. 1992, Nature, 359, 129
130. White, R. E., III, Keel, W. C., & Conselice, C. J. 1996, in New Extragalactic Perspectives in the New South Africa, ed. D.L. Block & J.M. Greenberg (Dordrecht: Kluwer), 114
131. White, R. E., III, Keel, W. C., & Conselice, C. J. 2000, ApJ, 542, 761
132. Witt, A. N., Lindell, R. S., Block, D. L., & Evans, R. 1994, ApJ, 427, 227
133. Xiang, F. Y., Li, A., & Zhong, J. X. 2011, ApJ, 733, 91
134. York, D. G., et al. 2006, MNRAS, 367, 945
135. Zasowski, G., Majewski, S. R., Indebetouw, R., et al. 2009, ApJ, 707, 510
136. Zhou, H., Ge, J., Lu, H., Wang, T., Yuan, W., Jiang, P., & Shan, H. 2010, ApJ, 708, 742

Penetrating the Dust Masks …

To David Block
my closest galactic companion

Mayo Geenberg

Jan 24 1996

星尘大师　　　　无尘道长

眼中有尘心无尘，除却雾霾无尘埃！
Young stars are born out of dust …

Congratulations on all the achievements, including in

Removing the dust masks …